MAGNETIC RESONANCE IN CHEMISTRY
Magn. Reson. Chem. **36**, 670–680 (1998)

Evaluation of the performance of 2D ^{1}H PFG absorption mode DQ spectroscopy in the analysis of chemical and biological molecules

Claudio Dalvit[1]* and Jean-Marc Böhlen[2]

[1] Novartis Pharma, CH-4002 Basle, Switzerland
[2] Bruker, CH-8117 Fällanden, Switzerland

Received 30 January 1998; revised 24 March 1998; accepted 9 April 1998

ABSTRACT: The performance of the ^{1}H 2D PFG-DQ experiment is analysed with theory and with some practical examples. The use of different angles for the detection pulse allows sensitivity optimization and spectral editing. Almost complete water suppression, high sensitivity, predominantly absorption lineshape, very low t_1 noise and absence of strong diagonal signals make the method very suitable for the analysis of complex mixtures, e.g. biofluids, cell cultures, natural product extracts and combinatorial chemistry samples. The method is also compared with the well known TOCSY and COSY experiments. © John Wiley & Sons Ltd.

KEYWORDS: NMR; ^{1}H NMR; double-quantum; pulsed-field gradients; solvent suppression; sensitivity; flip-angle dependence

INTRODUCTION

High-resolution proton NMR spectroscopy has become a useful tool for the investigation of biological and chemical systems.[1–3] The abundance of the ^{1}H nucleus in biomolecules and the non-destructive character of the method make possible the study of many compounds in their natural environment. Biofluids are particularly interesting systems, since they carry information about the state of the body. Another system which has become very important in the pharmaceutical industry is represented by combinatorial chemistry samples.

One of the most difficult tasks to achieve in the analysis of these systems by NMR spectroscopy is complete suppression of the water and other solvent signals. Excellent solvent suppression is critical in the analysis of molecules at micromolar concentrations. Solvent suppression allows the reduction of the dynamic range of the spectral peaks and thus makes possible the detection of signals of metabolites or drugs that are 5–8 orders of magnitude less intense than these otherwise dominant signals. The quality of the suppression also defines how close to the solvent frequency it is possible to detect signals. We recently proposed new ^{1}H 2D pulsed-field gradient (PFG) double-quantum (DQ or 2Q) experiments, which result in excellent solvent suppression and generate high-quality and high-sensitivity spectra devoid of t_1 noise and artifacts.[4,5] Two-dimensional ^{1}H DQ spectroscopy[6–9] provides essentially the same information as the 2D double-quantum filtered (DQF) COSY,[10] since it also correlates two protons that are scalar coupled. Except for *in vivo* applications, or in special editing techniques,[11–13] the DQ experiment has been almost ignored in high-resolution ^{1}H correlation spectroscopy to the benefit of the COSY-type experiments. The goal of the present work was to analyse the performance of the ^{1}H 2D PFG-DQ experiments and to show that there are some important advantages in their use.

* *Correspondence to*: C. Dalvit, Novartis Pharma, CH-4002 Basle, Switzerland.

EXPERIMENTAL

The experiments were recorded with Bruker Avance DMX-500 and DRX-600 spectrometers. The former was equipped with a triple-resonance inverse probe with an actively shielded *z*-gradient coil connected to a 10 A amplifier (100% amplitude corresponded to a gradient strength of 50.0 G cm^{-1}). The latter was equipped with an inverse ^{1}H/X probehead with an actively shielded three-axis gradient system and a triple gradient amplifier (3 × 10 A). The maximum achievable gradient strength at 100% amplitude was 50.5, 51.6 and 68.7 G cm^{-1} for the *x*, *y* and *z* directions, respectively.

The pulse sequence used for the 2D PFG-DQ experiments is shown in Fig. 1. The first three radiofrequency pulses create {2Q} coherences between spins that are scalar coupled. These coherences evolve during t_1 according to the sum of the frequencies of the two spins involved in the coherence. The read-out pulse β after t_1 partially converts the {2Q} coherences back into observable single-quantum {1Q} coherences. The last three PFGs are designed to select in the first experiment the anti-echo (N) pathway $\{-2Q\} \rightarrow \{-1Q\}$ and in the second experiment the echo (P) pathway $\{+2Q\} \rightarrow \{-1Q\}$. The sum of the echo and anti-echo data sets produces a cosine-modulated data set whereas

 CCC 0749-1581/98/090670–11 $17.50

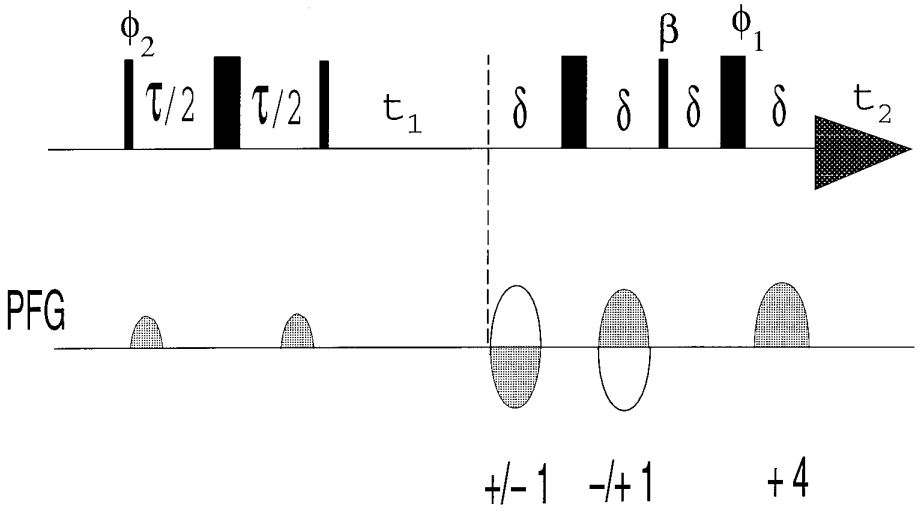

Figure 1. Pulse sequence of the ^{1}H 2D echo–antiecho PFG-DQ experiment. Narrow and wide bars correspond to 90° and 180° hard pulses, respectively. The angle β of the read-out pulse can be set to 90° (for both echo and anti-echo pathways) or to 30°/150°, 45°/135° or 60°/120° as described in the text. For the 90° version, the phases are $\phi_1 = 2(+x)$, $2(-y)$, $2(-x)$, $2(+y)$, $\phi_2 = (+x, -x)$ and $\phi_{rec} = (+x, -x, -x, +x)$. For the versions with $\beta \neq 90°$, the phases are $\phi_1 = (+x, -y, -x, +y)$ for both pathways, $\phi_2 = +x$ and $\phi_{rec} = (+x, -x)$ for the anti-echo pathway and $\phi_2 = -x$ and $\phi_{rec} = (-x, +x)$ for the echo pathway. A simply two-step phase-cycle is sufficient if concentrated molecules are studied. τ is the DQ excitation period and δ is a delay compensating for chemical shift dephasing during the last gradient. The coherence selection gradients (the last three in the scheme) are magic angle gradients (MAGs) for efficient solvent suppression, but can also be z-PFGs. The strength of these three gradients must obey the ratio $-1:+1:+4$ (or $+1:-1:-4$) for the anti-echo pathway selection and $+1:-1:+4$ (or $-1:+1:-4$) for the echo pathway selection. The data are processed with the so-called echo–antiecho mode.

its subtraction produces a sine-modulated data set.[14] These are then used for conventional SHR[15] processing. DQ spectra are generated where the direct correlation peaks have mostly an absorptive lineshape. Another reported version of the DQ experiment[16] makes use of coherence selection gradients and TPPI[17] for quadrature detection in ω_1. After phase-sensitive ω_1 calculation, a magnitude calculation was applied along ω_2. This experiment suffers a $\sqrt{2}$ sensitivity loss compared with the DQ experiment in Fig. 1.

RESULTS AND DISCUSSION

Suppression of solvents

In aqueous solutions, DQ experiments recorded with only the three coherence selection z-PFGs (the last three PFGs in Fig. 1) give spectra which contain a large residual H_2O signal. The origins of this undesired signal have been explained elsewhere.[18–26] Three improvements are possible on this basic experiment. (i) The water suppression is improved, when two weak PFGs are applied at the beginning and end of the period τ.[27] These do not simply serve to remove artefacts due to an imperfect 180° pulse, acting like an EXORCYCLE,[28,29] but more importantly they help to inhibit the creation of H_2O multiple-quantum coherence via radiation-damping effects during τ[18,27] and to ensure that the H_2O magnetization is aligned along the z-axis during the t_1 period. (ii) The radiofrequency phase of the first 90° pulse is set to x in the anti-echo version and $-x$ in the echo version of the PFG-DQ experiments recorded with $\beta \neq 90°$.[5] This is necessary in order to avoid the phenomenon of radiation damping during the acquisition period. (iii) Almost total water suppression is then obtained if three magic angle gradients (MAG) are used for the three coherence selection gradients.[4,5] At the magic angle ($\theta = 54.74°$ relative to the z-axis) the effect of the demagnetizing field is zero[19,22,23,26] and therefore antiphase H_2O magnetization present at the beginning of the acquisition period will not be refocused to observable in-phase magnetization.[22,24] This is demonstrated in Fig. 2 for a sample of blood plasma from a male Sprague–Dawley rat. The spectra have been obtained with the 1D version of the experiment of Fig. 1. The H_2O and β-glucose H-1 signals are plotted against increasing values of θ (angle of the gradient) crossing the magic angle value. The water signal diminishes and that of the glucose, located at about 0.1 ppm upfield from H_2O, remains unchanged, when approaching the magic angle orientation of the gradient (probably due to a small calibration inaccuracy, the experimental magic angle θ was 55.5°). The entire angle range spanned in Fig. 2 is only 2°. Note that a simple 1° decrease and increase in the angle θ from the magic angle results in seven- and five-fold increases in the residual H_2O signal, respectively.

An example of the ^{1}H 2D PFG-DQ experiment is shown in Fig. 3 for the α/β-glucose region. The 2D DQ spectrum of the biological plasma sample was recorded with the pulse sequences of Fig. 1 with $\beta = 90°$. Complete assignment is facilitated by the absence of diagonal peaks. Correlations between resonances with nearly

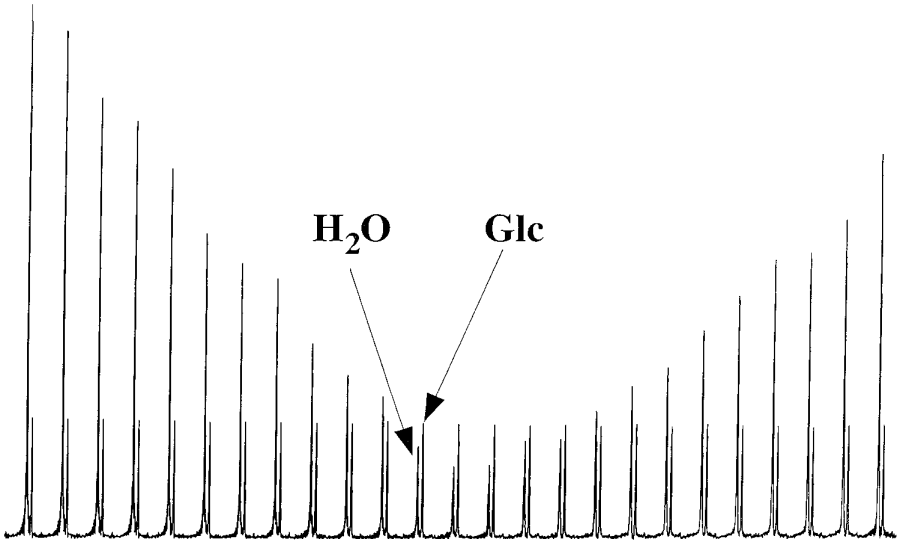

Figure 2. Calibration of the magic angle gradient condition. The experiments were recorded at $T_e = 296$ K with the Avance 600 spectrometer for a sample of blood plasma from a male Sprague–Dawley rat. The spectra were acquired with the 1D version of the pulse sequence of Fig. 1 with $\beta = 90°$, the first two gradients omitted, $t_1 = 10$ ms (corresponding to an intermediate value of the evolution period of a 2D experiment), $\tau = 30$ ms, an acquisition time of 250 ms and a repetition time of 2 s. The length of the three gradients was 1.5 ms and the recovery delay was set to 200 μs. A small portion of the blood plasma spectrum showing the residual water signal and the β-glucose H-1 signal, located at 0.1 ppm from H_2O, is displayed in magnitude mode. The z components of the three coherence selection gradients were kept fixed at +11.9, −11.9 and +47.6% throughout the measurements. The strengths of their x and y components were varied simultaneously from +15.85 to +17.05%, from −15.85 to −17.05% and from +63.4 to +68.2%. The increment for each step was 0.05, −0.05 and 0.2%, respectively. According to our gradient calibration, the changes in x and y components correspond to a total variation of θ by ±1% around the magic angle. One scan was recorded for each measurement. Note the improvement of the water suppression when approaching the right setting and the unchanged glucose signal.

identical chemical shifts can be observed. The spectrum also shows that β-glucose H-1 correlations may be observed without interference with the H_2O signal, which is reduced to the size of metabolite signals. In this spectrum the direct peaks are predominantly in absorption, with an in-phase character in the ω_1 dimension. These pairs of peaks are symmetrically disposed around the DQ pseudo-diagonal ($\omega_1 = 2\omega_2$). Remote peaks can be recognized owing to their opposite phase in the detection dimension and their asymmetric appearance around the DQ pseudo-diagonal. For example, in the 2D spectrum in Fig. 3, a remote peak (indicated by an arrow) is observed at the sum of the frequencies of β-H-1 and β-H-3 in ω_1 and at the frequency of β-H-2 in ω_2.

It has been shown that in addition to the H_2O signal the use of MAGs in DQ experiments results in excellent suppression of other solvent signals.[30,31] This is particularly important for the analysis of compounds dissolved in binary solvents such as H_2O–CH_3CN, H_2O–CH_3OH, H_2O–CH_3SOCH_3 or H_2O–CH_3COCH_3. For the acetone and DMSO solvents weak residual signals are observed at their centre frequency and at their ^{13}C satellite frequencies (see Fig. 3 in Ref. 30). The two CH_3 groups in acetone and DMSO are magnetically equivalent and therefore no {2Q} coherence can be created. However, this equivalence is removed in the molecules $^{13}CH_3SO^{12}CH_3$ and $^{13}CH_3CO^{12}CH_3$ and {2Q} coherence can now be created between the two CH_3 groups via the long-range proton scalar coupling ^4J. These residual signals can be eliminated from the spectrum by introducing a ^{13}C filter in the pulse sequence of Fig. 1.

Read-out pulse dependence

The efficency of conversion of the {2Q} coherence present during t_1 to observable anti-phase {1Q} coherence is dependent on the angle β of the read-out pulse.[7,32] This has been used recently to maximize the signal intensity in the ^{13}C–^{13}C INADEQUATE experiment.[33]

Let us consider a linear three-spin system composed of I_N, I_α and I_β spins of an amino acid moiety with the scalar couplings J_{N_α}, $J_{\alpha\beta} \neq 0$ and $J_{N_\beta} = 0$. We limit the analysis only to the $\{2Q\}_{N\alpha}$ and $I_\alpha{}^z\{2Q\}_{N\beta}$ terms present during t_1. At the end of t_1 the relevant terms are

$$[\{2Q\}^y_{N\alpha} \cos(\Omega_N + \Omega_\alpha)t_1 - \{2Q\}^x_{N\alpha} \sin(\Omega_N + \Omega_\alpha)t_1] \times [\cos \pi J_{\alpha\beta} t_1 \sin \pi J_{N\alpha} \tau(1 + \cos \pi J_{\alpha\beta} \tau)] \quad (1)$$

and

$$[I_\alpha{}^z\{2Q\}^x_{N\beta} \cos(\Omega_N + \Omega_\beta)t_1 + I_\alpha{}^z\{2Q\}^y_{N\beta} \sin(\Omega_N + \Omega_\beta)t_1] \times [\cos \pi(J_{N\alpha} + J_{\alpha\beta})t_1 \sin \pi J_{N\alpha} \tau \sin \pi J_{\alpha\beta} \tau] \quad (2)$$

The term in Eqn (1) is responsible for the observed direct peaks between the ^{N}H and $^\alpha$H spins whereas the term in Eqn (2) is responsible for the remote peak

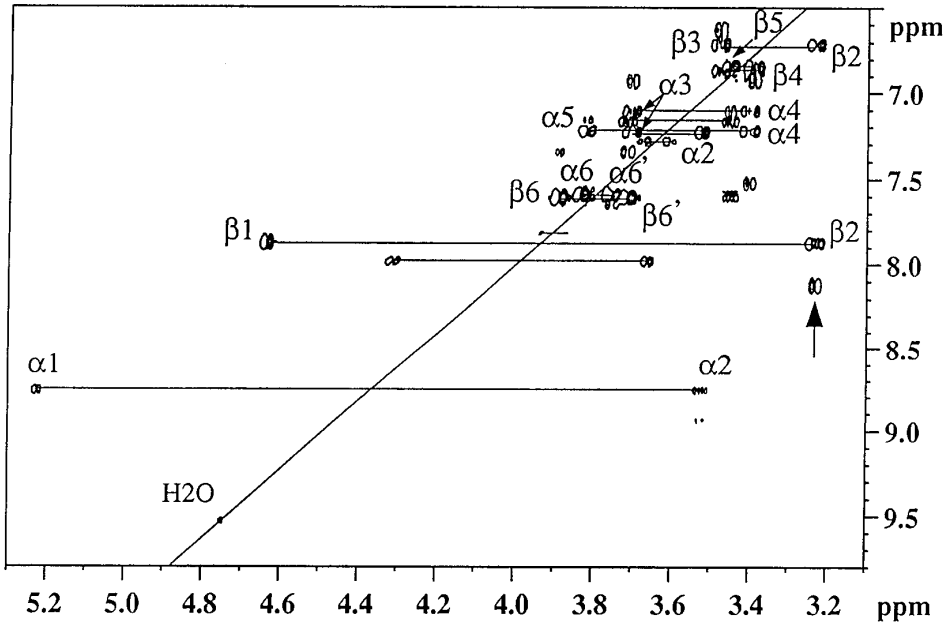

Figure 3. Glucose region of the 2D MAG DQ spectrum of the plasma sample recorded at $T_e = 296$ K with the Avance 600 spectrometer using the pulse sequence of Fig. 1 with $\beta = 90°$. Thirty-two scans were recorded for each of the 512 t_1 values (256 t_1 values for both echo and anti-echo sets). The ω_1 and ω_2 spectral widths were 16.0 and 10.0 ppm, respectively, and the acquisition time was 170 ms. The repetition time was 1.5 s, τ was 30 ms and the total experiment time was about 7 h. All the gradients were sine-shaped, had a duration of 1.5 ms and were followed by a 200 μs recovery time. The strength of the first two gradients was only 1%. The strengths of the three MAGs were $\mp$16.4, $\pm$16.4 and +65.6% for the *x* and *y* components, and $\mp$11.9, $\pm$11.9 and +47.6% for the *z* components. The gradient recovery delay was set to 200 μs. The data were multiplied with cosine square window functions in both dimensions prior to Fourier transformation. No treatment of the data was done for H_2O signal reduction. The residual H_2O signal is represented by the weak peak centred at $\omega_1 = 9.4$ ppm and $\omega_2 = 4.7$ ppm. The tilted line represents the DQ pseudo-diagonal and the horizontal lines connect the pairs of direct peaks which are symmetrically disposed with respect to the diagonal. Remote peaks (e.g. arrow) can be easily recognized since they appear only on one side of the DQ pseudo-diagonal and have the opposite phase in ω_2. Abbreviations are as follows: α_1–α_6, α-glucose H-1–H-6; β_1–β_6 : β-glucose H-1–H-6.

observed at the $^{\alpha}$H frequency and representing {2Q} coherence between the spins ^{N}H and $^{\beta}$H. If the angle β of the read-out pulse is set to 90° only the $\{2Q\}^{y}_{N\alpha}$ and $I_{\alpha}{}^{z}\{2Q\}^{x}_{N\beta}$ terms are partially converted to observable {1Q} coherence. For $\beta \neq 90°$ the term $\{2Q\}^{x}_{N\alpha}$ will also contribute to observable magnetization whereas the term $I_{\alpha}{}^{z}\{2Q\}^{y}_{N\beta}$ will never be made observable.

Because gradients are used for coherence selection, it is better to express Eqns (1) and (2) with the raising and lowering operators:[34]

$$\left[\frac{1}{2i}(I_N{}^{+}I_{\alpha}{}^{+} - I_N{}^{-}I_{\alpha}{}^{-})\cos(\Omega_N + \Omega_{\alpha})t_1 - \frac{1}{2}(I_N{}^{+}I_{\alpha}{}^{+} + I_N{}^{-}I_{\alpha}{}^{-})\sin(\Omega_N + \Omega_{\alpha})t_1\right] \times [\cos \pi J_{\alpha\beta} t_1 \sin \pi J_{N\alpha} \tau(1 + \cos \pi J_{\alpha\beta} \tau)] \quad (3)$$

$$\left[\frac{1}{2} I_{\alpha}{}^{z}(I_N{}^{+}I_{\beta}{}^{+} + I_N{}^{-}I_{\beta}{}^{-})\cos(\Omega_N + \Omega_{\beta})t_1 + \frac{1}{2i} I_{\alpha}{}^{z}(I_N{}^{+}I_{\beta}{}^{+} - I_N{}^{-}I_{\beta}{}^{-})\sin(\Omega_N + \Omega_{\beta})t_1\right] \times [\cos \pi(J_{N\alpha} + J_{\alpha\beta})t_1 \sin \pi J_{N\alpha}\tau \sin \pi J_{\alpha\beta}\tau] \quad (4)$$

The gradients select in one experiment the terms $I_N{}^{+}I_{\alpha}{}^{+}$, $I_{\alpha}{}^{z}(I_N{}^{+}I_{\beta}{}^{+})$, and in the other $I_N{}^{-}I_{\alpha}{}^{-}$, $I_{\alpha}{}^{z}(I_N{}^{-}I_{\beta}{}^{-})$

The conversion of these {2Q} terms to observable magnetization $I_N{}^{-}$ (direct peak) and $I_{\alpha}{}^{-}$ (remote peak) as a function of the angle β is then given by

$$I_N{}^{+}I_{\alpha}{}^{+} \rightarrow \beta I^{x} \rightarrow \frac{-i}{4}[I_N{}^{-}I_{\alpha}{}^{\alpha} - I_N{}^{-}I_{\alpha}{}^{\beta}] \sin \beta(\cos \beta - 1) \quad (5)$$

$$I_N{}^{-}I_{\alpha}{}^{-} \rightarrow \beta I^{x} \rightarrow \frac{-i}{4}[I_N{}^{-}I_{\alpha}{}^{\alpha} - I_N{}^{-}I_{\alpha}{}^{\beta}] \sin \beta(\cos \beta + 1) \quad (6)$$

$$I_{\alpha}{}^{z}I_N{}^{+}I_{\beta}{}^{+} \rightarrow \beta I^{x} \rightarrow \frac{i}{8}[I_{\alpha}{}^{-}I_N{}^{\alpha}I_{\beta}{}^{\alpha} - I_{\alpha}{}^{-}I_N{}^{\alpha}I_{\beta}{}^{\beta} - I_{\alpha}{}^{-}I_N{}^{\beta}I_{\beta}{}^{\alpha} + I_{\alpha}{}^{-}I_N{}^{\beta}I_{\beta}{}^{\beta}]\sin^3 \beta \quad (7)$$

$$I_{\alpha}{}^{z}I_N{}^{-}I_{\beta}{}^{-} \rightarrow \beta I^{x} \rightarrow \frac{i}{8}[I_{\alpha}{}^{-}I_N{}^{\alpha}I_{\beta}{}^{\alpha} - I_{\alpha}{}^{-}I_N{}^{\alpha}I_{\beta}{}^{\beta} - I_{\alpha}{}^{-}I_N{}^{\beta}I_{\beta}{}^{\alpha} + I_{\alpha}{}^{-}I_N{}^{\beta}I_{\beta}{}^{\beta}]\sin^3 \beta \quad (8)$$

The equation $I^z = \frac{1}{2}(I^\alpha - I^\beta)$ was used for deriving Eqns (5)–(8).

Plots of coherence transfer amplitude of {2Q} to {1Q} observable magnetization in the ^{1}H PFG echo–antiecho DQ experiment based on Eqns (5)–(8) are shown in Fig. 4. The relative signal intensity in the 90°/90°, 30°/150°, 45°/135° and 60°/120° versions of the experiment (normalized to the 90°/90° version) are for

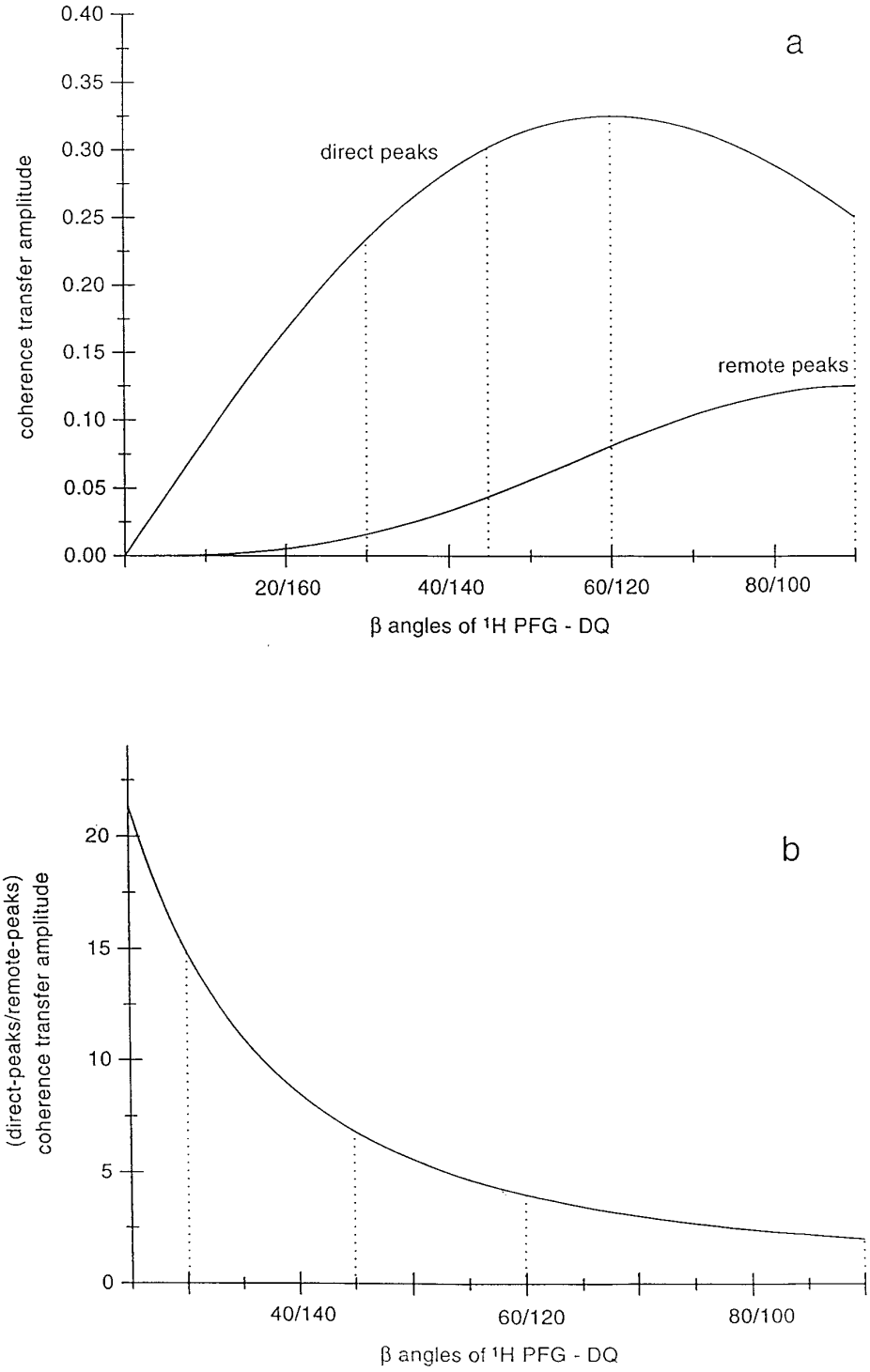

Figure 4. (a) Graph of the coherence transfer amplitude of {2Q} to observable {1Q} as a function of the angles of the read-out pulse used in the PFG-DQ experiments according to Eqns (5)–(8). The first value of the angle is used for the anti-echo pathway selection ($I^-I^- \rightarrow I^-$) and the second value is used for the echo pathway selection ($I^+I^+ \rightarrow I^-$). The vertical lines correspond to the different versions of the ^{1}H PFG-DQ experiment. Maximum values for the direct peaks and remote peaks are observed in the 60°/120° PFG-DQ and in the 90°/90° PFG-DQ experiments, respectively. (b) Graph of the coherence transfer amplitude direct peaks/remote peaks as a function of the angles of the read-out pulse used in the PFG-DQ experiments.

the direct peaks 1, 0.933, 1.207 and 1.299 and for the remote peaks 0.5, 0.062, 0.176 and 0.324, respectively [see Fig. 4(*a*)]. The coherence transfer amplitude direct peaks/remote peaks ratios, in the 90°/90°, 30°/150°, 45°/135° and 60°/120° versions of the experiment are 2, 14.92, 6.83 and 4, respectively [see Fig. 4(b)].

Figure 5 shows experimental results for (a) the direct peak at $\omega_1 = \omega_N + \omega_\alpha$ and $\omega_2 = \omega_N$ and (b) the remote peak at $\omega_1 = \omega_N + \omega_\beta$ and $\omega_2 = \omega_\alpha$ of the residue

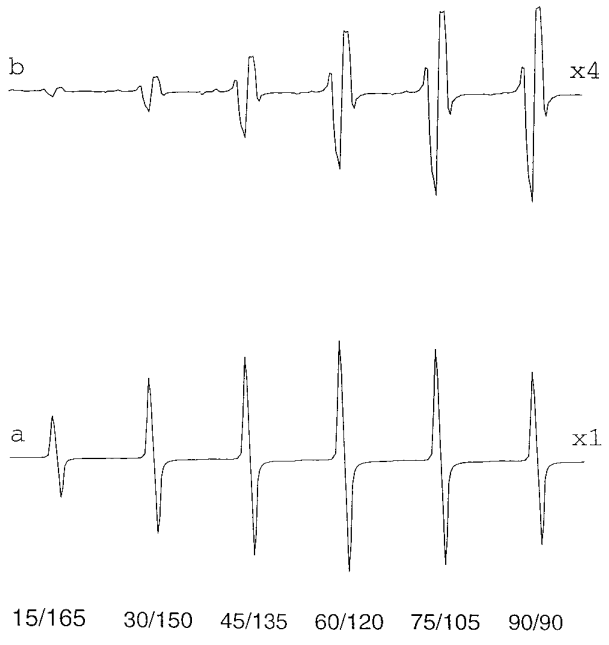

Figure 5. Experimental behaviour of the intensity of (a) the direct peak at $\omega_1 = \omega_N + \omega_\alpha$ (12.13 ppm) and $\omega_2 = \omega_N$ (7.47 ppm) and (b) the remote peak at $\omega_1 = \omega_N + \omega_\beta$ (9.90 ppm), $\omega_2 = \omega_\alpha$ (4.65 ppm) for the residue valine-5 as a function of the angles of the read-out pulse of the ^{1}H PFG-DQ experiment. The spectra in (b) were plotted at four times the level of the spectra in (a). The sample is the undecapeptide cyclosporin (CsA) dissolved in $CDCl_3$. The two peaks were extracted from six 2D ^{1}H PFG-DQ spectra recorded with the pulse sequence of Fig. 1 and with different angles for the detection pulse, as indicated in the figure. The experiments were recorded at $T_e = 297$ K with the Avance 500 spectrometer. Four scans were acquired for each of the 400 t_1 increments. The repetition time and the τ delay were 1.6 s and 30 ms, respectively. The ω_1 and ω_2 spectral widths were 14 and 8.8 ppm, respectively. The strength of the three sine-shaped PFGs of length 600 μs was ± 2.5, ∓ 2.5 and -10 G cm^{-1}, respectively and the gradient recovery time was 100 μs long. The data were multiplied in both dimensions with a cosine window function prior to 2D Fourier transformation. Note the absorptive single anti-phase lineshape for the direct peak and the dispersive doubly anti-phase lineshape for the remote peak. The strongest signal for the direct peak and for the remote peak are observed in the 60°/120° PFG-DQ and 90°/90° PFG-DQ experiments, respectively, in agreement with the theory. The 30°/150° PFG-DQ version achieves good intensity for the direct peak and strong attenuation for the remote peak.

valine-5 in the undecapeptide cyclosporin (CsA). The peaks were extracted from six 2D ^{1}H PFG-DQ experiments recorded with different angles for the read-out pulse. In agreement with the theory, the maximum signal for the direct peak and for the remote peak is observed for $\beta = 60°/120°$ and $\beta = 90°/90°$, respectively.

The version with $\beta = 60°/120°$ should be recorded when maximum sensitivity for the direct peaks is desired. This is important in the experiments where weak signals have to be detected, e.g. in e-PHOGSY-DQ experiments.[35] Figure 6 shows the fingerprint region of the 1–40 β-amyloid peptide recorded with the 60°/120° PFG-DQ experiment. The concentration of this sample was only 200 μM in order to avoid aggregation and the experimental measuring time was 7 h. Despite the low concentration, the intensity of the peaks in the DQ spectrum is high. A row containing the cross peak of M35, indicated by the arrow, shows clearly the large signal-to-noise (S/N) ratio. According to this spectrum it is evident that samples at concentrations of the order of 50 μM or even less could be analysed with this method. The $\beta = 30°/150°$ or $\beta = 45°/135°$ version should be used if attenuation of the remote peaks is desired. This may be useful for simplifying crowded spectral regions. Finally, the $\beta = 90°/90°$ version gives maximum intensity for the remote peaks. This is useful, for example, in the identification of the glycine spin systems in proteins. It should be pointed out that for more complex spin systems the use of a PFG-DQ experiment with $\beta \neq 90°$ results in the presence of some dispersive components. However, these are small and weak window functions can still be applied.

Sensitivity

Sensitivity comparison between different experiments is a difficult subject and often leads to controversy. The choice of experimental parameters influences differently the various types of experiments. Therefore, in the following analysis we used, as far as possible, the same experimental conditions.

Comparison with the ^{1}H 2D H_2O-pre-sat DQ experiment. The use of coherence selection gradients in the 90°/90° PFG-DQ experiment results in a $\sqrt{2}$ theoretical loss in sensitivity compared with the respective non-gradient DQ experiment, because the PFGs select in each data set only one of the two coherence pathways which can contribute to the observed signal.[14,36] However, the signal loss of the 60°/120° PFG-DQ experiment with respect to the TPPI DQ experiment is reduced to 1.088. This implies only an 18% increase in the measuring time of the PFG-DQ experiment in order to achieve the same S/N ratio obtained with the non-gradient DQ version.

However, experimental factors contribute to the superior performance of the PFG version. Phase cycling, which is a method based on difference spectroscopy, is used in the non-gradient DQ experiment to

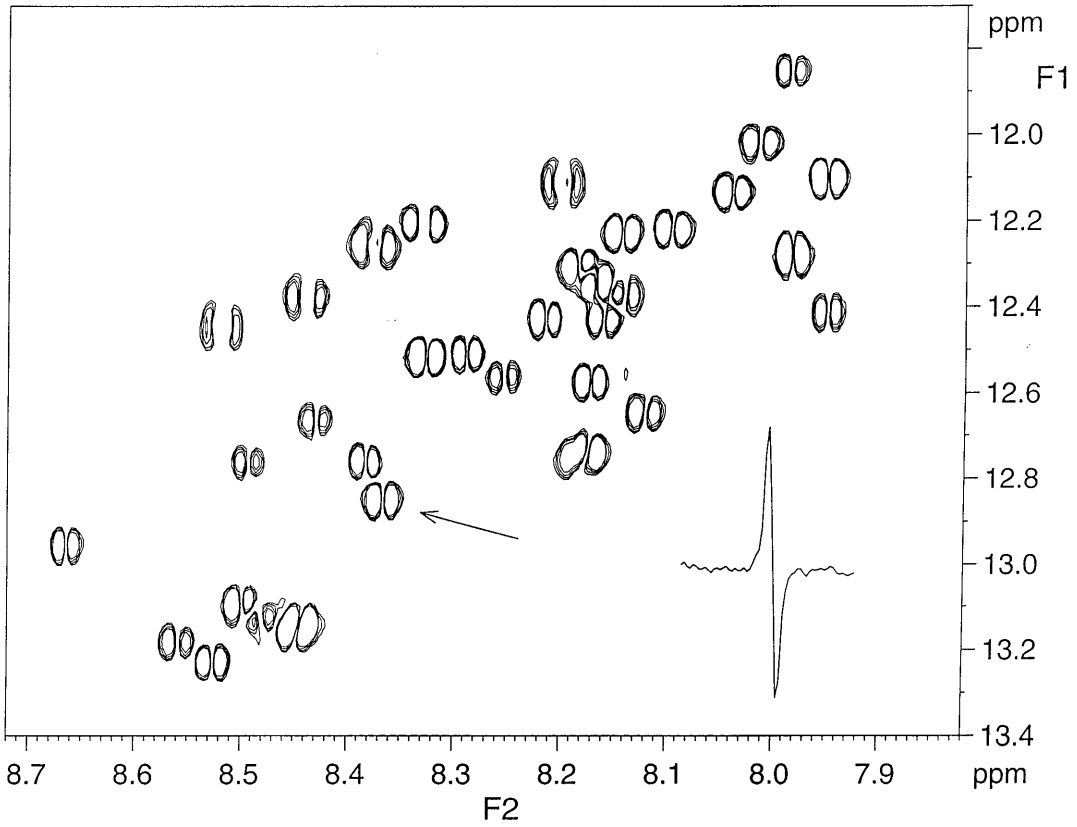

Figure 6. Fingerprint region of the DQ spectrum of the 1–40 amyloid peptide in H_2O (5% D_2O) recorded with the pulse sequence of Fig. 1 with $\beta = 60°/120°$. The peptide concentration was 200 μM and the pH of the solution was 2.9. The spectrum was recorded at $T_e = 297$ K with the Avance 500 spectrometer. Thirty-two scans were recorded for each of the 512 t_1 increments. The repetition time was 1.6 s, τ was 30 ms and the total measuring time was about 7 h. The ω_1 and ω_2 spectral widths were 16 and 8.8 ppm, respectively. The strength of the first two 1.25 ms long sine-shaped PFGs was + 0.35 G cm^{-1}. The strength of the three 0.6 ms long coherence selection PFGs was ± 5, ∓ 5 and -20 G cm^{-1}, respectively. The gradient recovery time was 100 μs. The data were multiplied in both dimensions with a cosine window function prior to 2D Fourier transformation. The 1D cross-section taken at the cross peak of M35, indicated by the arrow, is displayed in order to show the S/N ratio.

select the proper coherence pathway. Owing to various instabilities the resulting spectra contain some residual t_1 noise originating from improper cancellation of the undesired magnetization. This problem is not encountered in the PFG-DQ version because the gradients select in every transient only the desired coherence pathway.[14,36–38] Therefore, the limit of signal detection in the PFG-DQ experiment is determined solely by the thermal noise and not by the t_1 noise. Furthermore, for samples dissolved in H_2O other factors contribute to the better performance of the PFG-DQ experiment. The use of H_2O presaturation in the standard DQ experiment has several negative effects. First the irradiation of H_2O and the large residual t_1 noise of H_2O do not allow the detection of the solute peaks resonating at or close to the H_2O signal. The observation of these resonances is particularly important in DQ spectra of biomolecules for tracing the different spin systems. Other negative effects are shown with two examples in Fig. 7. Two rows in the amide regions are extracted from the 2D PFG-DQ (a, c) and the 2D DQ with H_2O irradiation (b, d) experiments recorded for the protein chicken egg white lysozyme dissolved in H_2O (7% D_2O). The spectra were recorded using the same experimental parameters and are displayed at the same level. The signal improvement for some resonances in the PFG-DQ spectra is striking. The main disadvantages of using H_2O irradiation is that the resonances close to the H_2O signal are partially saturated by the r.f. field and that saturation transfer may partially saturate fast exchangeable NH resonances. $\{2Q\}_{N_\alpha}$ coherence is created starting from both ^{N}H and $^{\alpha}H$ spins. Therefore, saturation of one or both of these spins will result in a reduced amount of $\{2Q\}_{N_\alpha}$ coherence. This is the case, for example, for the resonances of I88 and T118 in Fig. 7. The $^{\alpha}H$ signals of these residues resonate at the H_2O chemical shift. Saturation transfer can also yield signal attenuation via an indirect process. The H_2O saturation results equally in saturation of the OH protons of Tyr, Ser and Thr. During the long irradiation period, which is typically 1–2 s, the magnetization of the OH spins will migrate via cross-relaxation to other protons close in space. The final result is again a signal reduction of these spins. This is in part the case for the resonance of S50 in Fig. 7. The ^{N}H and $^{\alpha}H$ spins of S50 have reduced intensity at the beginning of the DQ excitation period owing to the intraresidual NOE experienced originating from the OH spin.

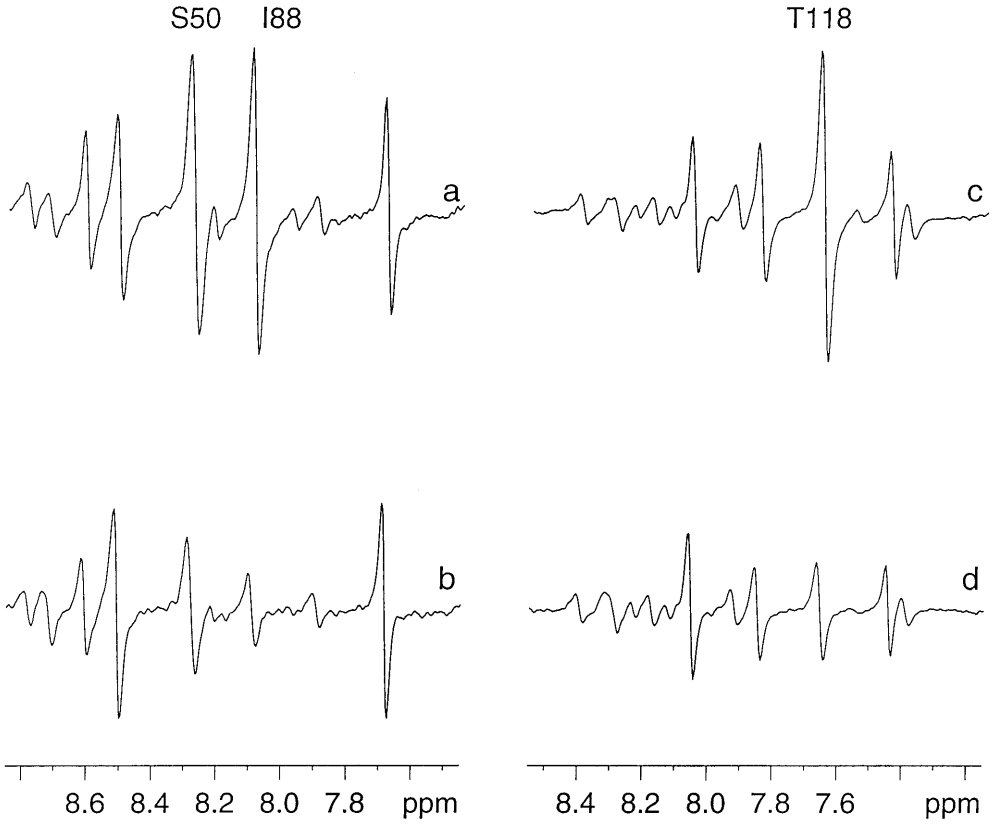

Figure 7. Two rows extracted from 45°/135° PFG-DQ (a, c) and H_2O-pre-sat DQ (b, d) spectra recorded for a 6 mM solution of chicken-egg-white lysozyme dissolved in H_2O (7% D_2O) and at pH 3.8. The rows were taken at $\omega_1 = 12.82$ ppm (a, b) and at $\omega_1 = 12.38$ ppm (c, d). The spectra were plotted at the same level. The DQ signals present in these rows originate from $\{2Q\}_{N_z}$. Only the amide region is displayed. The spectra were acquired and processed with the same experimental parameters. The experiments were recorded at $T_e = 297$ K with the Avance 500 spectrometer. Sixteen scans were acquired for each of the 300 t_1 increments. The repetition time and the τ delay were 1.65 s and 30 ms, respectively. The length of the H_2O presaturation period was 1.4 s and the strength of the r.f. field was 50 Hz in the DQ experiment with H_2O irradiation. The ω_1 and ω_2 spectral widths were 16.8 and 9.4 ppm, respectively. In the PFG-DQ experiment the strength of the first two 1.25 ms long sine-shaped PFGs was $+0.85$ G cm^{-1} and the strength for the three 0.6 ms long sine-shaped coherence selection gradients was ± 5, ∓ 5 and -20 G cm^{-1}, respectively. The gradient recovery time was 100 μs. The data were multiplied with a cosine window function in both dimensions prior to Fourier transformation. The NH of I88, S50 and T118 (assignment taken from Ref. 53) are labelled. The sensitivity improvement in the PFG-DQ *vs.* DQ with H_2O irradiation experiment is 2.0, 4.2, 3.1 S50, I88 and T118, respectively.

Comparison with the ^{1}H 2D H_2O-pre-sat COSY experiment. The COSY experiment is in theory twice as sensitive as the DQ experiment. However, as explained clearly in Ref. 3, the performance of the COSY experiment is strongly dependent on some practical parameters. First, the digital resolution in t_1 is critical in the COSY experiment for determining the relative cross peak intensity. Low digital resolution in ω_1 results in partial cancellation of the positive and negative lobes of the cross peaks with a consequent reduction of the signal intensity. Second, the COSY experiment is a so-called sine-modulated experiment due to its $\sin \pi J t_1$ dependence. As a result, a large number of t_1 increments is required if cross peaks are to be observed. In contrast, DQ experiments are cosine-modulated experiments and consequently the maximum signal is observed in the first t_1 increments. DQ experiments can be recorded rapidly by acquiring only a small number of t_1 increments. Linear prediction can then be applied in the t_1 dimension for improving the frequency resolution. Note also that DQ, owing to its predominantly in-phase character in ω_1, is suitable for establishing scalar connectivities by way of small long-range couplings.

Figure 8 shows two rows extracted from ^{1}H PFG-DQ and ^{1}H COSY with H_2O irradiation experiments recorded for the biological plasma sample. These rows contain the signals of the amino acids Ala (a) and Tyr (b) which are found in biological plasma. The two 2D PFG-DQ spectra were recorded with read-out pulse $\beta = 45°/135°$ and 90°/90° (the two spectra on the left). The COSY spectrum was acquired with the same measuring time and processed with two different window functions (the two spectra on the right). The peaks with the highest S/N ratio are observed in the DQ spectra.

Another experiment that achieves excellent H_2O suppression by employing magic angle gradients[39,40] is the PFG-DQF-COSY.[41] Experimental comparison of the PFG DQ and PFG-DQF-COSY experiments has been reported previously.[30]

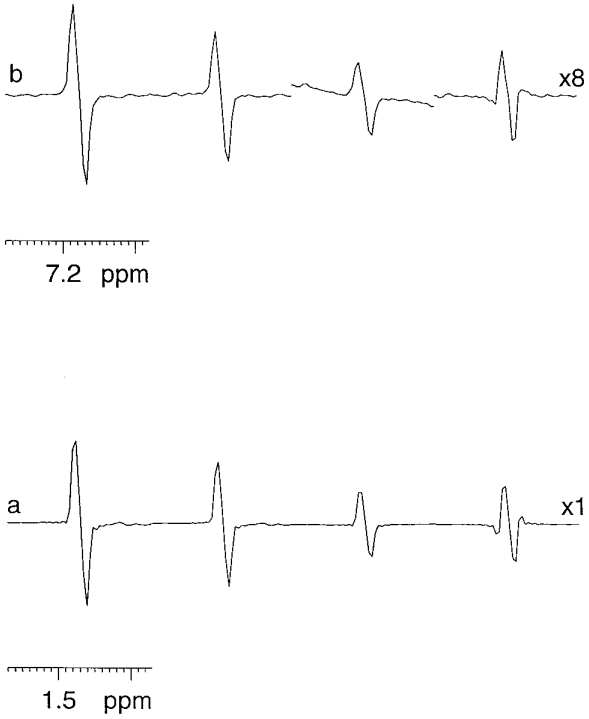

Figure 8. Two rows extracted from 2D spectra recorded for th sample of rat blood plasma. The cross peaks are for the amino acids (a) Ala and (b) Tyr. The cross-section originated from left to right from 2D 45°/135° PFG-DQ, 90°/90° PFG-DQ and two differently processed H_2O-pre-sat COSY spectra. The spectra were plotted at the same level. The scale tick spacing corresponds to 0.01 ppm. The experiments were recorded at $T_e = 297$ K with the Avance 500 spectrometer. Sixteen scans with a repetition time of 1.65 s were recorded for each of the 512 t_1 increments. The length of the H_2O presaturation period was 1.4 s and the strength of the r.f. field was 50 Hz. The ω_2 spectral width was 9.4 ppm and the ω_1 spectral width was 9.4 and 16.8 ppm for the H_2O-pre-sat COSY and PFG-DQ experiments, respectively. The excitation DQ period τ and the gradient recovery time were 32 ms and 100 μs, respectively. The strength of the five 1.25 ms long sine-shaped PFGs was +0.35, +0.35, ±5, ∓5 and −20 G cm^{-1}, respectively. The three spectra on the left were processed with the same cosine window functions applied in both dimensions. The COSY spectrum on the right was processed in both dimensions with 3° shifted sine-bell window functions. The use of this strong window function matches best the detected COSY signal. The relative intensity of the cross peaks normalized to the cross peak intensity in the 90°/90° PFG-DQ spectrum are for both Ala and Tyr from left to right 1.3, 1.0, 0.5 and 0.6, respectively.

Comparison with ^{1}H 2D TOCSY experiments. A cosine-modulated experiment which provides information about the spin system networks is the TOCSY experiment.[42,43] The version of this experiment with the WATERGATE scheme[44] is used for the analysis of samples dissolved in H_2O. The intensity of a TOCSY cross peak depends on all the couplings within a spin system. TOCSY experiments with short isotropic mixing periods are recorded in order to ensure magnetization transfer through a single scalar coupling interaction and therefore giving information similar to the COSY and DQ experiments. However, the presence of zero-quantum artifacts in these spectra, especially for small and medium-sized molecules, distort severely the cross peaks. The use of z-filters[45] or of a spin-lock pulse combined with a gradient[46] at the end of the TOCSY experiment will partially reduce this effect. For long mixing periods the ROE transfer which is of opposite sign of the TOCSY transfer will attenuate the TOCSY cross peaks between two spins which are close in space. The use of 'clean' isotropic mixing sequences[47] suppresses this effect in TOCSY experiments of large molecules. Its use cannot be extended to small molecules because the NOEs and ROEs in small molecules have the same sign.

Figure 9 shows three cross peaks extracted from two ^{1}H 2D PFG-DQ recorded with readout pulse $\beta = 45°/135°$ and 90°/90° (left) and three 2D WATERGATE-TOCSY (right) spectra recorded for the biological plasma sample. The DQ cross peaks for the small molecules Ala (a) and Tyr (b) are clearly more intense than the respective TOCSY cross peaks. However, for large molecules such as the VLDL particles in plasma (c) the TOCSY cross peaks are more intense than the DQ cross peaks. The TOCSY cross peaks are in-phase in both dimensions whereas the DQ cross peaks are predominantly in-phase in ω_1 and anti-phase in ω_2. The large half-height width of the VLDL CH_3 resonance (30 Hz) decreases the intensity of the DQ cross-peak owing to the partial cancellation of the positive and negative lobes along ω_2. A method for avoiding this problem is the use of a refocused PFG-DQ experiments.[31,48] The peaks are in-phase in these spectra and therefore no signal losses occur via cancellation. However, the use of the additional refocusing period results in signal losses via T_2 relaxation and incomplete conversion of the anti-phase magnetization to in-phase magnetization.

The spectra on the furthest right in Fig. 9 deserve some comments. An experiment which has been proposed for determining the diffusion coefficient of a molecule is the so-called stimulated-echo TOCSY experiment.[49–51] A stimulated-echo scheme is applied before the TOCSY step. The cross peaks on the right are extracted from a stimulated-echo TOCSY spectrum recorded with the same isotropic-mixing period as in the TOCSY spectrum second from right. The bipolar diffusion gradients in the stimulated-echo scheme select only one of the two possible coherence pathways, resulting in a twofold signal loss. This is clearly seen in Fig. 9(a) and (b). In this comparison we have used intentionally weak bipolar diffusion gradients in order to exclude signal attenuation due to diffusion occurring in the time between the rising edges of the two bipolar gradients. For large molecules the extra delays of the stimulated-echo scheme result in additional signal losses via T_1 and T_2 relaxation as seen in Fig. 9(c). The two PFGs in the DQ excitation period can also be used to measure the diffusion coefficient of a molecule or to distinguish molecules based on their differential diffusion

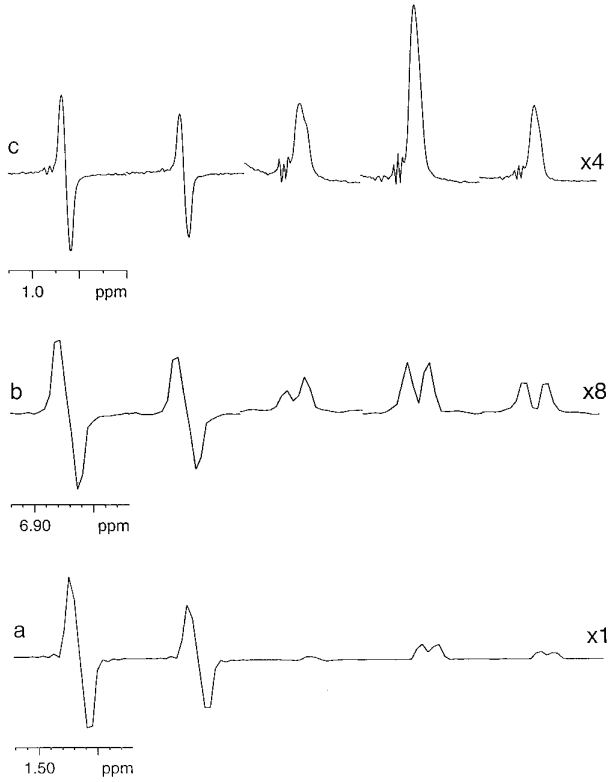

Figure 9. Three rows extracted from 2D spectra recorded for the sample of biological plasma. The cross peaks are for the amino acids (a) Ala and (b) Tyr and (c) for the VLDL particles. The cross-sections are from left to right from 2D 45°/135° PFG-DQ, 90°/90° PFG-DQ, WATERGATE-TOCSY with $\tau = 15$ ms, WATERGATE-TOCSY with $\tau = 31$ ms and WATERGATE-stimulated-echo-TOCSY with $\tau = 31$ ms. The τ period represents the length of the spin-locking period. The spectra were plotted at the same level. The scale tick spacing corresponds to 0.01 ppm in (a) and (b) and 0.1 ppm in (c). The experiments were recorded at $T_e = 297$ K with the Avance 500 spectrometer. Sixteen scans with a repetition time of 1.65 s were recorded for each of the 400 t_1 increments. The ω_2 spectral width was 9.4 ppm and the ω_1 spectral width was 9.4 and 16.8 ppm for the TOCSY and PFG-DQ experiments, respectively. The other acquisition parameters were the same as in Fig. 8. In the stimulated-echo TOCSY experiment the delay between the start of the two bipolar gradients comprising the stimulated-echo scheme was 31 ms. The length of the two sine-shaped bipolar gradients and the gradient recovery time were 1.25 ms and 100 μs, respectively. Their strength was set to the low value of |0.35| G cm^{-1} in order to avoid signal attenuation due to spatial diffusion and thus allowing a direct comparison with the other experiments. The relative cross peak intensities normalized to the cross peak of the 90°/90° PFG-DQ spectrum are from left to right in (a) 1.4, 1.0, 0.1, 0.3 and 0.2, in (b) 1.3, 1.0, 0.6, 1.0 and 0.5 and in (c) 1.3, 1.0, 1.0, 3.1 and 1.3.

coefficients.[31,52] This is achieved within the pulse sequence of Fig. 1 without the use of additional delays and pulses. Furthermore, the PFGs in the DQ excitation period are not used for coherence selection and therefore all the magnetization is refocused at the end of τ. The diffusion-weighted DQ spectra can also be displayed in magnitude mode along ω_2 for facilitating quantitation of the signal intensities. A drawback of the experiment of Fig. 1 is that molecules which produce ^{1}H NMR spectra with only singlets cannot be studied. Despite this disadvantage, the diffusion-weighted phase-sensitive DQ experiment compares favourably with other diffusion-weighted experiments.

CONCLUSION

We have shown that ^{1}H 2D PFG phase-sensitive DQ experiments represent a powerful method for the study of molecules dissolved in non-deuterated solvents. The experiment is not simply a helpful complement to other correlation experiments. The excellent solvent suppression achieved with this experiment and its intrinsic high sensitivity allow the detection of low-concentration molecules. It could become a method of choice in LC–NMR and in the analysis of biological systems and of combinatorial chemistry samples.

Acknowledgements

We thank Dr Francis Bitsch for providing us with the sample of biological plasma from a male Sprague–Dawley rat and Dr Staufenbiel for the 1–40β amyloid peptide sample. Thanks are due to Dr R. Richmond for helpful discussions.

REFERENCES

1. K. Wüthrich, *NMR of Proteins and Nucleic Acids*, Wiley, New York (1986).
2. I. Bertini and C. Luchinat, *NMR of Paramagnetic Molecules in Biological Systems*. Benjamin/Cummings, Menlo Park, CA (1986).
3. J. Cavanagh, W. J. Fairbrother, A. G. Palmer, III and N. J. Skelton, *Protein NMR Spectroscopy*. Academic Press, New York (1996).
4. C. Dalvit and J. M. Böhlen, *J. Magn. Reson. B* **111**, 76 (1996).
5. C. Dalvit and J. M. Böhlen, *J. Magn. Reson. B* **113**, 195 (1996).
6. T. H. Mareci and R. Freeman, *J. Magn. Reson.* **51**, 531 (1983).
7. L. Braunschweiler, G. Bodenhausen and R. R. Ernst, *Mol. Phys.* **48**, 535 (1983).
8. M. Rance and P. E. Wright, *J. Magn. Reson.* **66**, 372 (1986).
9. T. J. Norwood, *Prog. Nucl. Magn. Reson. Spectrosc.* **24**, 295 (1992).
10. M. Rance, O. W. Sørensen, G. Bodenhausen, G. Wagner, R. R. Ernst and K. Wüthrich, *Biochem. Biophys. Res. Commun.* **117**, 479 (1983).
11. C. H. Sotak, D. M. Freeman and R. E. Hurd, *J. Magn. Reson.* **78**, 355 (1988).
12. R. E. Hurd and D. M. Freeman, *Proc. Natl. Acad. Sci. USA* **86**, 4402 (1989).
13. W. Nosel, L. A. Trimble, J. F. Shen and P. S. Allen, *Magn. Reson. Med.* **11**, 398 (1989).
14. J. Keeler, R. T. Clowes, A. L. Davis and E. D. Laue, *Methods Enzymol.* **239**, 145 (1994).
15. D. J. States, R. A. Haberkorn and D. J. Ruben, *J. Magn. Reson.* **48**, 286 (1982).
16. J. Balbach and H. Kessler, *J. Magn. Reson. B* **105**, 83 (1994).
17. D. Marion and K. Wüthrich, *Biochem. Biophys. Res. Commun.* **113**, 967 (1983).
18. M. McCoy and W. S. Warren, *J. Chem Phys.* **93**, 858 (1990).
19. R. Bowtell, R. M. Bowley and P. Glover, *J. Magn. Reson.* **88**, 643 (1990).
20. D. Abergel, M. A. Delsuc and J. Y. Lallemand, *J. Chem. Phys.* **96**, 1657 (1992).
21. W. S. Warren, Q. He, M. McCoy and F. C. Spano, *J. Chem. Phys.* **96**, 1659 (1992).

22. W. S. Warren, W. Richter, A. H. Andreotti and B. T. Farmer, II, *Science* **262**, 2005 (1993).
23. R. Bowtell and A. Peters, *J. Magn. Reson. A.* **115**, 55 (1995).
24. S. Lee, W. Richter, S. Vathyam and W. S. Warren, *J. Chem. Phys.* **105**, 874 (1996).
25. P. Broekaert, A. Vlassebroek, J. Jeener, G. Lippens and J. M. Wieruszeski, *J. Magn. Reson. A.* **120**, 97 (1996).
26. M. Levitt, *Concepts Magn. Reson.* **8**, 77 (1996).
27. C. Dalvit and J. M. Böhlen, *J. Magn. Reson.* **126**, 149 (1997).
28. G. Bodenhausen, R. Freeman and D. L. Turner, *J. Magn. Reson.* **27**, 511 (1977).
29. A. Bax and S. S. Pochapsky, *J. Magn. Reson.* **99**, 638 (1992).
30. C. Dalvit and J. M. Böhlen, *Magn. Reson. Chem.* **34**, 829 (1996).
31. C. Dalvit and J. M. Böhlen, *NMR Biomed.* **10**, 285 (1997).
32. T. H. Mareci and R. Freeman, *J. Magn. Reson.* **48**, 158 (1982).
33. N. C. Nielsen, H. Thøgersen and O. W. Sørensen, *J. Am. Chem. Soc.* **117**, 11365 (1995).
34. R. R. Ernst, G. Bodenhausen and A. Wokaun, *Principles of Nuclear Magnetic Resonance in One and Two Dimensions.* Clarendon Press, Oxford (1987).
35. C. Dalvit, *J. Magn. Reson. B* **112**, 282 (1996).
36. G. Kontaxis, J. Stonehouse, E. D. Laue and J. Keeler, *J. Magn. Reson. A* **111**, 70 (1994).
37. D. Canet and M. Decorps, in *Dynamics of Solutions and Fluid Mixture by NMR*, edited by J. J. Delpuech, p. 310. Wiley, New York (1995).
38. T. Parella, *Magn. Reson. Chem.* **34**, 329 (1996).
39. P. C. M. Van Zijl, M. O. Johnson, S. Mori and R. E. Hurd, *J. Magn. Reson. A* **113**, 265 (1995).
40. D. L. Mattiello, W. S. Warren, L. Müller and B. T. Farmer, II, *J. Am. Chem. Soc.* **118**, 3253 (1996).
41. A. L. Davis, E. D. Laue, J. Keeler, D. Moskau and J. Lohman, *J. Magn. Reson.* **94**, 637 (1991).
42. L. Braunschweiler and R. R. Ernst, *J. Magn. Reson.* **53**, 521 (1983).
43. A. Bax and D. G. Davis, *J. Magn. Reson.* **65**, 355 (1985).
44. M. Piotto, V. Saudek and V. Sklenar, *J. Biomol. NMR* **2**, 661 (1992).
45. O. W. Sørensen, M. Rance and R. R. Ernst, *J. Magn. Reson.* **56**, 527 (1984).
46. A. L. Davis, G. Estcourt, J. Keeler, E. D. Laue and J. J. Titman, *J. Magn. Reson. A* **105**, 167 (1993).
47. C. Griesinger, G. Otting, K. Wüthrich and R. R. Ernst, *J. Am. Chem. Soc.* **110**, 7870 (1988).
48. M. Rance, O. W. Sørensen, W. Leupin, H. Kogler, K. Wüthrich and R. R. Ernst, *J. Magn. Reson.* **61**, 67 (1985).
49. A. Jerschow and N. Müller, *J. Magn. Reson. A* **123**, 222 (1996).
50. M. Liu, J. K. Nicholson and J. C. Lindon, *Anal. Chem.* **68**, 3370 (1996).
51. M. Lin and M. J. Shapiro, *J. Org. Chem.* **61**, 7617 (1996).
52. N. Birlirakis and G. Guittet, *J. Am. Chem. Soc.* **118**, 13083 (1996).
53. C. Redfield and C. M. Dobson, *Biochemistry* **27**, 122 (1988).

